Received: 8 February 2020 | Revised: 10 March 2020 | Accepted: 20 March 2020

DOI: 10.1002/mgg3.1245

ORIGINAL ARTICLE

Molecular Genetics & Genomic Medicine Open Access WILEY

Bioinformatics analysis and verification of gene targets for benign tracheal stenosis

Xu-ze Li[1] | Zi-chen Wang[1] | Yong Qiu[2] | Shu-xian Ma[1] | Ling-bing Meng[3] | Wen-hao Wu[1] | Pei Zhang[1] | Wei Yang[4] | Wen-ping Song[4] | Lining Huang[1]

[1]Department of Anesthesiology, The Second Hospital of Hebei Medical University, Shijiazhuang, China

[2]Anesthesiology Department, Beijing Hospital, National Center of Gerontology, Beijing, P. R. China

[3]Neurology Department, Beijing Hospital, National Center of Gerontology, Beijing, P. R. China

[4]Shandong Weigao Group National Engineering Lab, Weihai, China

Correspondence
Lining Huang, Department of Anesthesiology, The Second Hospital of Hebei Medical University, No. 215, Heping West Road, Xinhua District, Shijiazhuang 050000, China.
Email: 15803213730@163.com

Funding information
Discipline Leader Training Program of Hebei Provincial Government; Chinese Academy of Sciences-Wego Group Hightech Research & Development Program

Abstract

Background: Tracheal injury could cause intratracheal scar hyperplasia which in turn causes benign tracheal stenosis (TS). With the increasing use of mechanical ventilation and ventilator, the incidence of TS is increasing. However, the molecular mechanisms of TS have not been elucidated. It is significant to further explore the molecular mechanisms of TS.

Methods: The repeatability of public data was verified. Differently expressed genes (DEGs) and most significant genes were identified between TS and normal samples. Enrichment analysis of Gene Ontology (GO) and Kyoto Encyclopedia of Genes and Genomes (KEGG) were analyzed. The comparative toxicogenomics database were analyzed. TS patients were recruited and RT-qPCR were performed to verify the most significant genes.

Results: There exist strong correlations among samples of TS and normal group. There was a total of 194 DEGs, including 61 downregulated DEGs and 133 up-regulated DEGs. GO were significantly enriched in mitotic nuclear division, cell cycle, and cell division. Analysis of KEGG indicated that the top pathways were cell cycle, and p53 pathway. *MKI67(OMIM:176741)*, *CCNB1(OMIM:123836)*, and *CCNB2(OMIM:602755)* were identified as the most significant genes of TS, and validated by the clinical samples.

Conclusion: Bioinformatics methods might be useful method to explore the mechanisms of TS. In addition, *MKI67*, *CCNB1*, and *CCNB2* might be the most significant genes of TS.

KEYWORDS

bioinformatic, cell cycle, differentially expressed genes, tracheal stenosis

Xu-ze Li and Zi-chen Wang contributed to the paper equally.

1 | INTRODUCTION

Tracheal stenosis (TS) refers to the reduction in diameter of the trachea, caused by tracheotomy, intratracheal tumors, tracheomalacia, infections, inflammations, and other pathologic conditions (Farzanegan et al., 2017; Raghuraman, Rajan, Marzouk, Mullhi, & Smith, 2005). What is more, most cases of TS develop as a result of tracheal intubation or tracheostomy which induce intratracheal scar hyperplasia (Kim, Khalpey, Hsu, & Little, 2017). A retrospective study of 150 patients with TS showed that 54.7% of the cases are caused by iatrogenic injury, 18.5% are caused by autoimmune, and 8% are caused by trauma (Gelbard et al., 2015). In addition, with the increasing use of mechanical ventilation and ventilator, the incidence of TS is increasing (Ahn, Su, Kim, & I H., 2015). Due to dyspnea, patients' quality of life is badly affected. When symptoms are severe, surgical intervention is warranted (Farzanegan et al., 2017).

Multiple mechanisms are involved in tracheal stenosis, but the molecular mechanisms remain unclear. The endotracheal tube cuff excessively compresses the tracheal wall, causing mucosal injury and inflammatory response, which in turn induces tracheal wall damage and scar formation (Su et al., 2017). Meanwhile, inflammatory cells and immune cells caused by tracheal wall damage secrete a variety of inflammatory factors and growth factors such as IL-6 which can promote fibrous scar formation (Yin et al., 2017). Furthermore, resection of the stenotic lesions, balloon dilation, and stenting are the main treatments to relieve stenosis (D'Andrilli, Venuta, & Rendina, 2016). However, the surgical treatment itself might also cause new tracheal injury and anastomotic complications, inducing new fibrous scar (Wright et al., 2019). Generally, early diagnosis and management for the TS could bring a better prognosis to the patients (Smith & Cotton, 2018). Therefore, it is significant to further explore the mechanisms of TS and find molecular targets that can be used to diagnose early, prevent early, and treat early.

Bioinformatics methods are widely used to find molecular changes in the occurrence and development of diseases and are effective ways to explore the pathogenesis of diseases. Zhang found the genes related to the pathogenesis of oralsquarous cell carcinoma (OSCC) utilizing bioinformatics analysis, and further verified these molecules might lead to OSCC through the PI3K-AKT pathway, suggesting the relevant molecules may be a molecular target for specific diagnosis and therapy (Zhang, Feng, et al., 2018; Zhang, Zhang, et al., 2018). In addition, Liu found abnormally expressed molecules in multiple scar tissues by bioinformatics analysis and further verified that *SFRP1(OMIM:604156)* might take part in the occurrence of scar by regulating Wnt/β-catenin (Liu et al., 2018). However, there are few reports on the use of bioinformatics analysis to explore the mechanisms of acute tracheal injury and TS.

Plenty of DEGs were identified between TS and control individuals via the bioinformatics analysis. Enrichment analysis was implemented. Furthermore, the research constructed networks of Protein-protein Interaction (PPI), significant modules, and hub genes. Finally, three most significant genes (*MKI67(OMIM:176741)*, *CCNB1(OMIM:123836)*, and *CCNB2(OMIM:602755)*) were identified and verified by the functional experiment of the clinical samples.

2 | MATERIALS AND METHODS

2.1 | Obtaining the public data

The GEO (http://www.ncbi.nlm.nih.gov/geo) is an open source platform for the storage of genetic data (Edgar, Domrachev, & Lash, 2002). One expression profiling dataset [GSE109365 (GPL16570 platform)] were downloaded. The GSE109365 dataset (Musah et al., 2019) includes five tracheal stenosis samples which were exposed to chlorine 4 days, and five normal trachea which were not exposed to chlorine.

2.2 | The repeatability test for the intra-group data

The repeatability of data was verified by the Pearson's correlation test. R (Lin et al., 2017) is an open language and environment for statistical computing and mapping, which was maintained by a large and active global research community. The Pearson's correlation test and the mapping of heat maps were completed by the R language. Principal component analysis (PCA; Ringner, 2008), a strong mathematical method, was capable of reducing the data's complexity. The PCA could capture variance in the whole fields by detecting the linear combinations, so that the components, which were orthogonal to and not correlated with each other, were divided. Also, the repeatability of data was verified by the PCA.

2.3 | Differently expressed genes (DEGs) identified by LIMMA package

As a fully functional package, the LIMMA package includes the original data input and preprocessing capabilities of chips, as well as a liner model for analyzing differentially expressed genes. We screened DEGs between normal and TS samples by utilizing LIMMA package with a adjust $p < .001$ and a log (Fold Change) ≥ 1 or log (Fold Change) ≤ -1. And the volcano plot was drawn by R language. The DEGs are presented as volcano plots, generated using SangerBox software (http://sangerbox.com/).

2.4 | Construction of a PPI network

Search Tool for the Retrieval of Interacting Genes (http://string.embl.de/; Szklarczyk et al., 2015), an open source online tool, was used to construct a PPI network, and Cytoscape visualization software version 3.6.1(Smoot, Ono, Ruscheinski, Wang, & Ideker, 2011) was implemented to complete visualization. A confidence score >0.4 was set, which may filter out the critical module.

2.5 | GO and KEGG analysis via DAVID tool

One online tool, DAVID (Huang et al., 2007; https://david.ncifcrf.gov/home.jsp; version 6.8, Maryland, America), was applied to carried out the functional annotation for DEGs. GO (Ashburner et al., 2000) generally perform enrichment analysis of genomes. And there are mainly cellular components (CC), biological processes (BP), and molecular functions (MF) in the GO analysis. KEGG (https://www.kegg.jp/; Tanabe & Kanehisa, 2012) is a comprehensive database of genomic, chemical, and systemic functional information. Therefore, DAVID was used to make analysis of GO and KEGG.

2.6 | Enrichment analysis by Metascape

Metascape (http://metascape.org/gp/index.html#/main/step1; Zhou et al., 2019) is a powerful annotation analysis tool for gene function, which can help researchers apply the current popular bioinformatics analysis methods to the analysis of batch genes and proteins, so as to realize the cognition of gene or protein functions. It can annotate a large number of genes or proteins. It integrates several authoritative functional databases, such as GO, KEGG, and Uniprot, to analyze not only human data, but also the data of many other species, and to analyze not only a single dataset, but also multiple gene sets simultaneously. The Matascape was performed.

2.7 | The screening of significant module, and identification of hub genes

Molecular Complex Detection tool (MCODE; version 1.5.1; Bader & Hogue, 2003), one plug-in of Cytoscape, could screen and identify the most significant module in the PPI network, and the criteria were given as the degree of cut-off = 2, MCODE scores > 5, *k*-score = 2, node score cut-off = 0.2, and maximum depth = 100. Furthermore, once the degree was more than 10, the cytoHubba (Chin et al., 2014), one plug-in of Cytoscape, could identify the hub genes.

2.8 | The analysis of hub genes

The R was used to perform the clustering analysis based on the gene expression level. The Pearson's correlation test was performed to complete the correlation analysis among the hub genes. And the mapping of heat maps, which could present the correlation among the all hub genes, were completed by the R language.

2.9 | The validation of most significant genes

The MCC algorithm of cytoHubba was also implemented to identify the hub genes. And the VENN was used to obtain the common genes between “cytoHubba_Degree” and “cytoHubba_MCC.” Then, the most significant genes were identified.

2.10 | Identification of the most significant genes associated with trachea

The comparative toxicogenomics database (http://ctdbase.org/) is a web-based tool that provides their relationships with diseases. The relationships between the significant genes and “Tracheal Diseases, Cartilage Diseases, Tracheal Neoplasms, Fibroadenoma, and Connective Tissue Diseases” were analyzed via comparative toxicogenomics database.

2.11 | Ethical compliance

The research conformed to the Declaration of Helsinki and was authorized by the Human Ethics and Research Ethics Committees of the Second Hospital of Hebei Medical University. All participates provided the informed consents.

2.12 | Patients

This study recruited a total of 25 individuals including 11 TS patients and 14 un-TS individuals between 2017 and 2020 from the Second Hospital of Hebei Medical University. There was no difference in tube duration, and the balloon pressure was monitored during tube duration, and the pressure was within the clinically acceptable range. Clinical characteristics and basic information were available for all patients, and were collected retrospectively from medical records. Patients aged 18–100 years old, suspected tracheal stenosis TS based on symptom, not received treatment, and no history of tracheal surgery will be screened for inclusion criteria. Exclusion criteria included: age <18 years old or

>100 years old, combined with other malignant diseases, and severs heart disease and diabetes.

2.13 | RT-qPCR assay

RNAiso Plus (Trizol) kit (Thermofisher) was implemented to extracte RNA of the most significant genes, including *MKI67* (Reference Sequence: NG_047061.1), *CCNB1* (Reference Sequence: NC_000005.10), *CCNB2* (Reference Sequence: NC_000015.10). Light Cycler® 4800 System was used to make RT-qPCR for the 10 hub genes. The primer sequences are presented in Table 1. The relative quantitative values (ΔCT) were calculated. The endogenous control was GAPDH.

2.14 | Statistical analysis

The data were expressed as percentage of total and mean ± *SD*. Student's *t* test was used to compare value between two groups.

By using the Pearson's correlation test, associations between the degree of TS and the expression of *MKI67*, *CCNB1*, and *CCNB2* were analyzed. And we used the linear regression analysis to explore the linear correlations between them. The Spearman-rho test was used to compare degree of TS, the expression of *MKI67*, *CCNB1*, and *CCNB2* for the correlation analysis.

3 | RESULTS

3.1 | High repeatability of data in the GSE109365

There existed strong relevance among individuals in TS group, and in the normal individuals in the GSE109365 via the Pearson's correlation test (Figure 1a). Furthermore, through the PCA, the repeatability of the data in GSE109365 was fine (Figure 1b).

TABLE 1 Primers and their sequences for PCR analysis

Primer	Sequence (5′–3′)
MKI67-hF	GCTCACGCCTGTAATCCC
MKI67-hR	TGCTCTTCGCTTTGCTTT
CCNB1-hF	GTGTTCTAACTTTGGAGGAT
CCNB1-hR	TCAGTCACCCAATACCAG
*CCNB*2-hF	TAATGGGCATTTCTGTAAG
*CCNB*2-hR	CAGGGCTATTGTTTGGTA

Note: MKI67 (Reference Sequence: NG_047061.1), *CCNB1* (Reference Sequence: NC_000005.10), *CCNB2* (Reference Sequence: NC_000015.10).

3.2 | DEGs between TS and normal samples and the PPI network

There was a total of 194 DEGs between TS and normal samples, including 61 downregulated DEGs and 133 upregulated DEGs. The volcano plot presents the DEGs in the GSE10 9365 (Figure 1c). And the PPI network was constructed (Figure 1d).

3.3 | Functional annotation for DEGs via DAVID

The BP were mainly enriched in mitotic nuclear division, cell cycle, cell division, chromosome segregation, mitotic cytokinesis, and positive regulation of fibroblast proliferation (Figure 2a). The CC were mainly enriched in chromosome, centromeric region, and condensed chromosome kinetochore (Figure 2b). The MF were significantly enriched in cyclin binding, ATPase activity, and growth factor activity. (Figure 2c). Result of KEGG analysis showed that top pathways were cell cycle, p53 signaling pathway, TNF signaling pathway, cytosolic DNA-sensing pathway, Oocyte meiosis (Figure 2d).

3.4 | The analysis of metascape

Furthermore, the functional enrichment analysis with Metascape manifested that the DEGs between TS and un-TS samples were significantly enriched in mitotic cell cycle process, cytokinetic process, cell cycle, formation of the cornified envelope, monocyte chemotaxis, meiotic nuclear division, cytosolic DNA-sensing pathway, SUMOylation of DNA replication proteins, inflammatory response, negative regulation of proteolysis, chromosome condensation, regulation of growth, ovulation, protein localization to cytoskeleton ($p < .05$, Figure 2e–g).

3.5 | The identification of significant module

Four significant modules were also identified by the MCODE (Figure 3a–d).

3.6 | The identification and analysis of hub genes

The 10 hub genes were identified by "cytoHubba" (Figure 4a). Heatmap showed that hub genes could differentiate the TS and un-TS samples. When compared with un-TS samples, the hub genes were upregulated in the TS samples (Figure 4b).

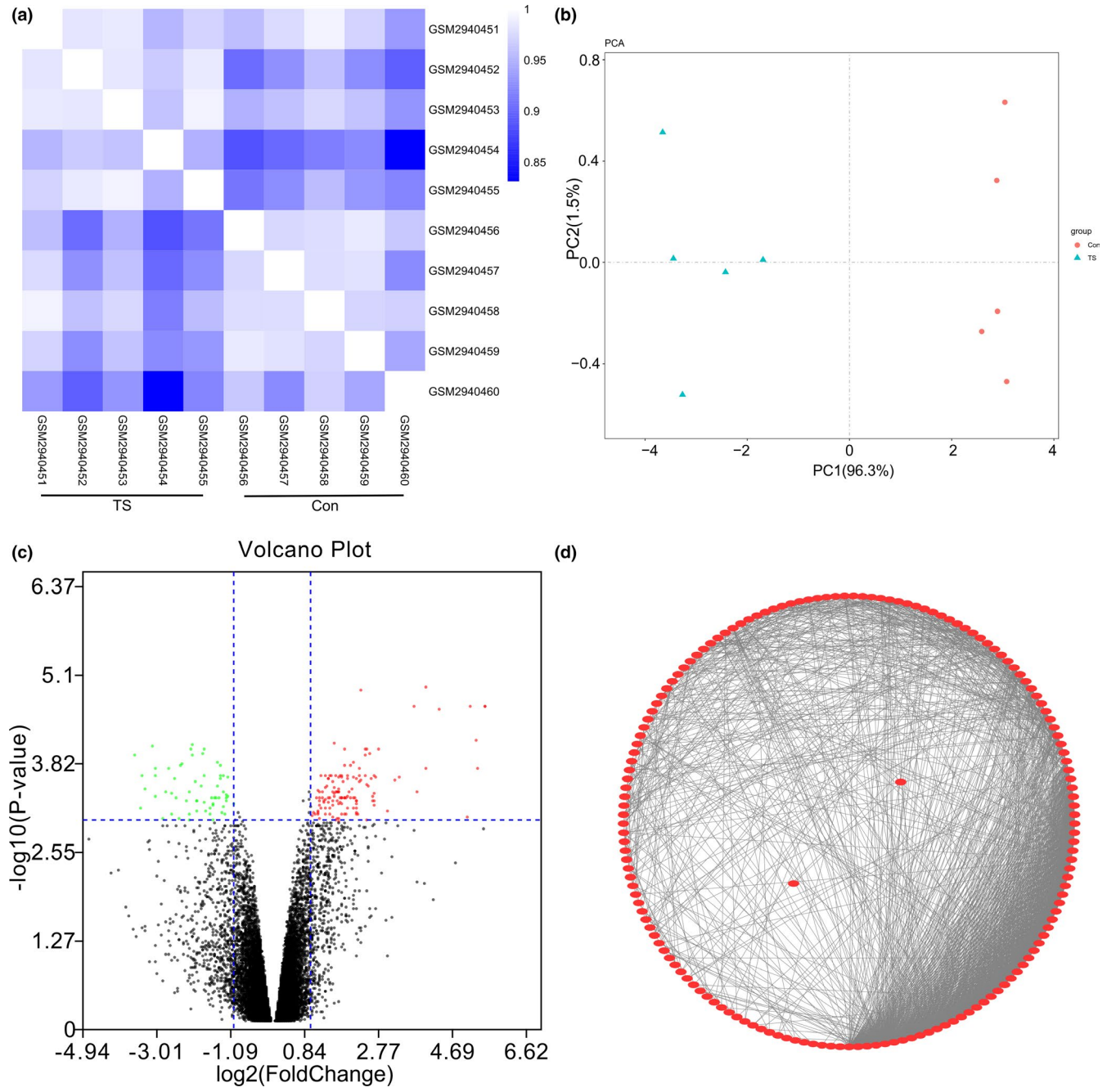

FIGURE 1 (a) Pearson's correlation test manifests that there exist powerful correlations among samples in the TS group, and that there also exist powerful correlations among samples in control group in the GSE109365 dataset. (b) After performing the principal component analysis, the repeatability of data in GSE109365 was fine. (c) Volcano plot presents the DEGs between TS and control groups. (d) PPI network of the DEGs

The Pearson correlation analysis manifested that there exist positive correlations among all the hub genes (Figure 5a).

3.7 | The most significant genes

After analysis of MCC, 10genes were selected from PPI network (Figure 5b). The VENN diagram showed that there were three most significant genes (*Mki67*, *Ccnb1*, *Ccnb2*) between "cytoHubba_Degree" and "cytoHubba_MCC" (Figure 5c).

3.8 | The CTD analysis of most significant genes

Identification of significant genes associated with tracheal diseases, cartilage diseases, tracheal neoplasms, fibroadenoma,

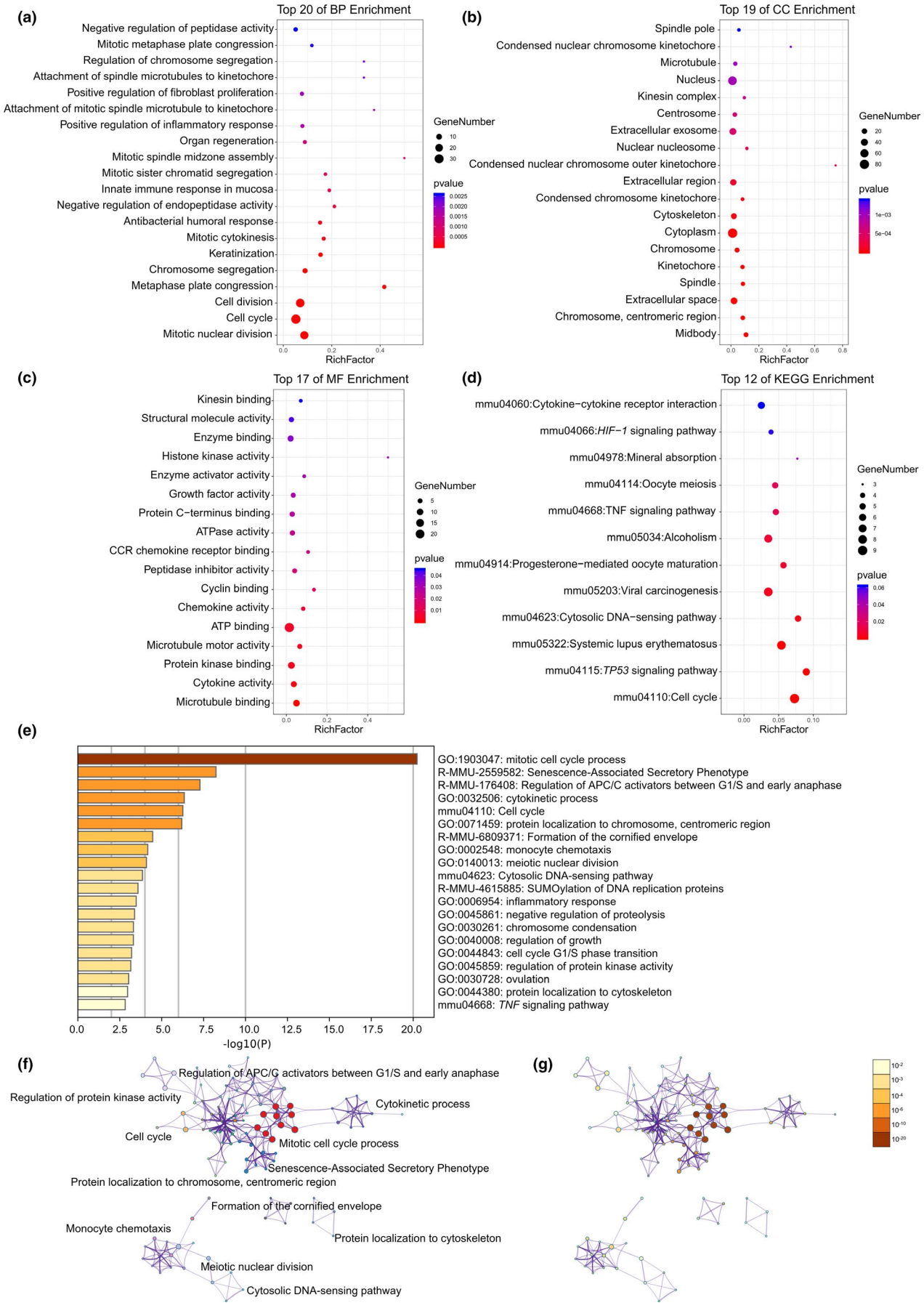
(a)
Top 20 of BP Enrichment
Negative regulation of peptidase activity
Mitotic metaphase plate congression
Regulation of chromosome segregation
Attachment of spindle microtubules to kinetochore
Positive regulation of fibroblast proliferation
Attachment of mitotic spindle microtubule to kinetochore
Positive regulation of inflammatory response
Organ regeneration
Mitotic spindle midzone assembly
Mitotic sister chromatid segregation
Innate immune response in mucosa
Negative regulation of endopeptidase activity
Antibacterial humoral response
Mitotic cytokinesis
Keratinization
Chromosome segregation
Metaphase plate congression
Cell division
Cell cycle
Mitotic nuclear division
RichFactor
GeneNumber
pvalue
(b)
Top 19 of CC Enrichment
Spindle pole
Condensed nuclear chromosome kinetochore
Microtubule
Nucleus
Kinesin complex
Centrosome
Extracellular exosome
Nuclear nucleosome
Condensed nuclear chromosome outer kinetochore
Extracellular region
Condensed chromosome kinetochore
Cytoskeleton
Cytoplasm
Chromosome
Kinetochore
Spindle
Extracellular space
Chromosome, centromeric region
Midbody
RichFactor
GeneNumber
pvalue
(c)
Top 17 of MF Enrichment
Kinesin binding
Structural molecule activity
Enzyme binding
Histone kinase activity
Enzyme activator activity
Growth factor activity
Protein C−terminus binding
ATPase activity
CCR chemokine receptor binding
Peptidase inhibitor activity
Cyclin binding
Chemokine activity
ATP binding
Microtubule motor activity
Protein kinase binding
Cytokine activity
Microtubule binding
RichFactor
GeneNumber
pvalue
(d)
Top 12 of KEGG Enrichment
mmu04060:Cytokine−cytokine receptor interaction
mmu04066:HIF−1 signaling pathway
mmu04978:Mineral absorption
mmu04114:Oocyte meiosis
mmu04668:TNF signaling pathway
mmu05034:Alcoholism
mmu04914:Progesterone−mediated oocyte maturation
mmu05203:Viral carcinogenesis
mmu04623:Cytosolic DNA−sensing pathway
mmu05322:Systemic lupus erythematosus
mmu04115:TP53 signaling pathway
mmu04110:Cell cycle
RichFactor
GeneNumber
pvalue
(e)
-log10(P)
GO:1903047: mitotic cell cycle process
R-MMU-2559582: Senescence-Associated Secretory Phenotype
R-MMU-176408: Regulation of APC/C activators between G1/S and early anaphase
GO:0032506: cytokinetic process
mmu04110: Cell cycle
GO:0071459: protein localization to chromosome, centromeric region
R-MMU-6809371: Formation of the cornified envelope
GO:0002548: monocyte chemotaxis
GO:0140013: meiotic nuclear division
mmu04623: Cytosolic DNA-sensing pathway
R-MMU-4615885: SUMOylation of DNA replication proteins
GO:0006954: inflammatory response
GO:0045861: negative regulation of proteolysis
GO:0030261: chromosome condensation
GO:0040008: regulation of growth
GO:0044843: cell cycle G1/S phase transition
GO:0045859: regulation of protein kinase activity
GO:0030728: ovulation
GO:0044380: protein localization to cytoskeleton
mmu04668: TNF signaling pathway
(f)
Regulation of APC/C activators between G1/S and early anaphase
Regulation of protein kinase activity
Cytokinetic process
Cell cycle
Mitotic cell cycle process
Senescence-Associated Secretory Phenotype
Protein localization to chromosome, centromeric region
Formation of the cornified envelope
Monocyte chemotaxis
Protein localization to cytoskeleton
Meiotic nuclear division
Cytosolic DNA-sensing pathway
(g)

FIGURE 2 The enrichment analysis of DEGs by DAVID and Metascape. Detailed information relating to changes in the (a) CC, (b) BP, (c) MF, and (d) KEGG analysis for hub genes. (e) Heatmap of enriched terms across input differently expressed gene lists, colored by *p*-values, via the Metascape. (f) Network of enriched terms colored by cluster identity, where nodes that share the same cluster identity are typically close to each other. (g) Network of enriched terms colored by *p*-value, where terms containing more genes tend to have a more significant *p*-value

and connective tissue diseases was performed on CTD database which is shown in Figure 5d–f. Specifically, the *MKI67* is shown in Figure 5d, the *CCNB1* in Figure 5e, and the *CCNB2* in Figure 5f.

3.9 | Patient characteristics

The demographic data and the expression status of *MKI67*, *CCNB1*, and *CCNB2* are summarized in the Table 2. The mean patient age was 54 years (range, 25–85 years).

3.10 | RT-qPCR analysis validation of the most significant genes (*MKI67*, *CCNB1*, and *CCNB2*)

As presented in the result, the expression of *MKI67* ($p < .05$, Figure 6a), *CCNB1* ($p < .05$, Figure 6b), and *CCNB2* ($p < .05$, Figure 6c) were significantly upregulated in TS samples. It should be noted that the expression situation of *MKI67*, *CCNB1*, and *CCNB2* were consistent in above bioinformatic results. The degree of TS in the TS group was higher (Figure 6d).

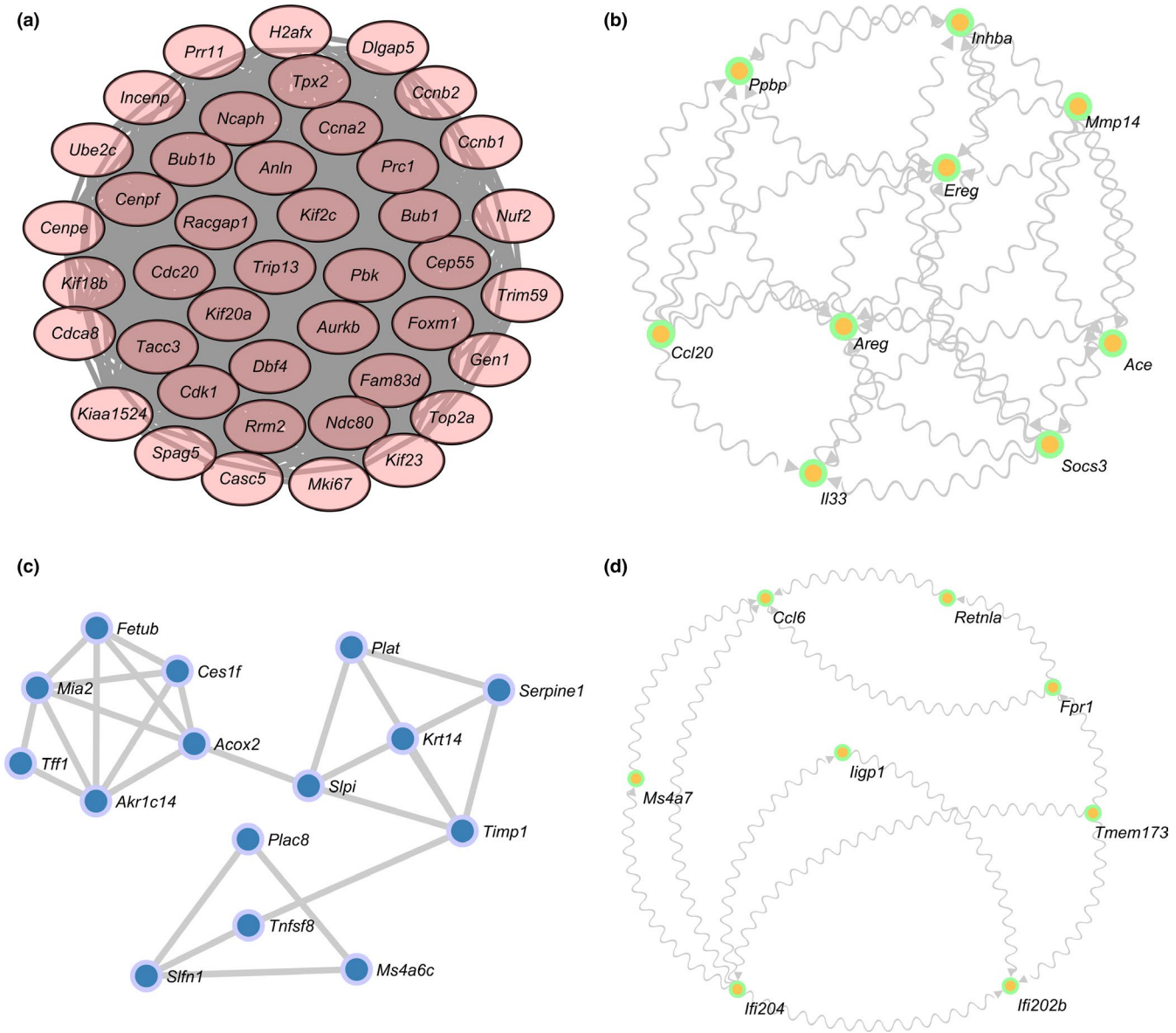

FIGURE 3 The four significant modules identified from the PPI network

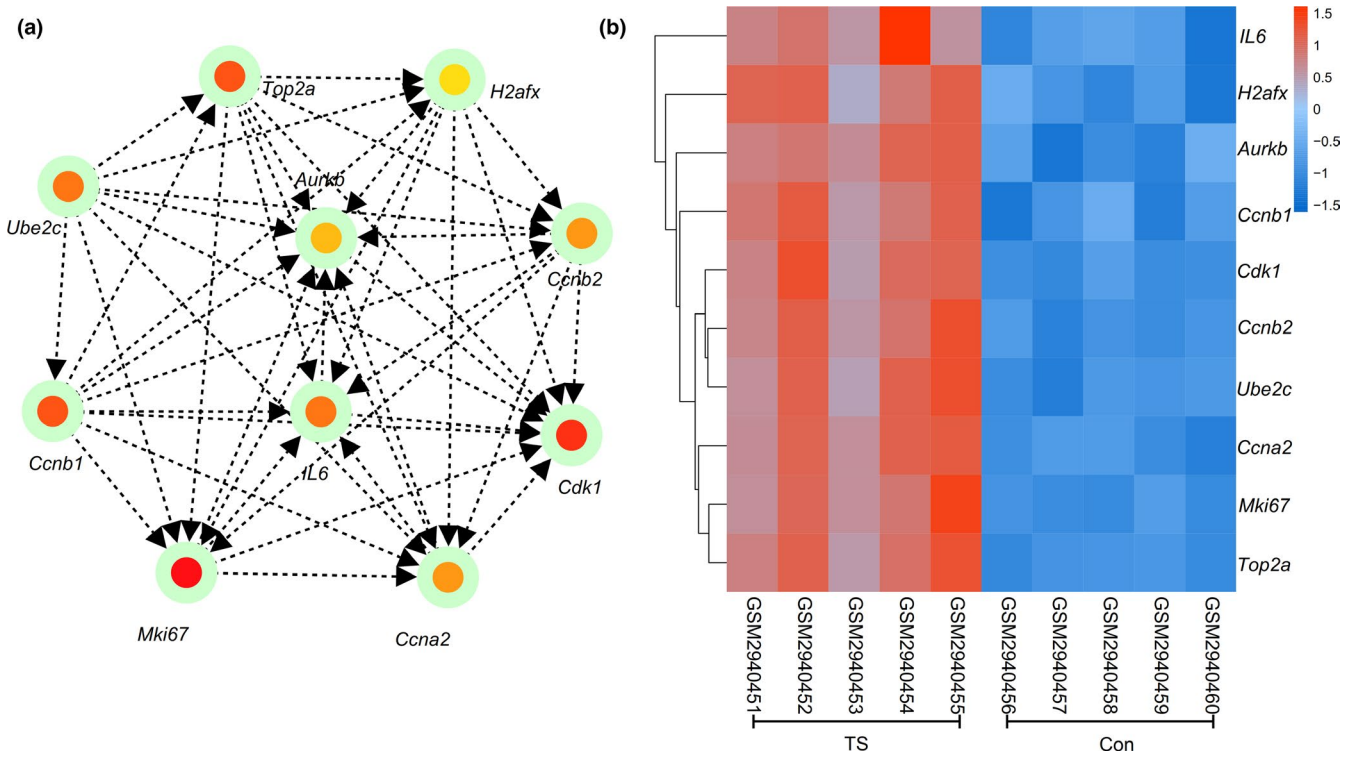

FIGURE 4 The hub genes network via cytoHubba_Degree (a), and the heatmap presenting the expression of these hub genes (b)

3.11 | Strong positive associations between the degree of TS, *MKI67*, *CCNB1*, and *CCNB2*

The degree of TS was positively associated with the *MKI67* ($R = .906$, $p < .001$; Figure 7a). And the degree of TS was positively related with *CCNB1* ($R = .953$, $p < .001$; Figure 7b). The degree of TS was positively associated with the *CCNB2* ($R = .958$, $p < .001$; Figure 7c). And *MKI67* was positively associated with *CCNB1* ($R = .912$, $p < .001$; Figure 7d). The relative expression of *MKI67* was positively related with *CCNB2* ($R = .862$, $p < .001$; Figure 7e). *CCNB1* was positively associated with *CCNB2* ($R = .936$, $p < .001$; Figure 7f). The heatmap showed the strong associations between the *MKI67*, *CCNB1*, and *CCNB2* through the Spearman correlation analysis (Figure 8).

4 | DISCUSSION

Tracheal injury can cause intratracheal scar hyperplasia which in turn causes TS (Farzanegan et al., 2017). With the increasing use of mechanical ventilation and ventilator, the incidence of TS is increasing (Kim et al., 2017). What is more, Patients with TS may experience symptoms such as dyspnea, wheezing, and other symptoms and their life and work are seriously affected (Farzanegan et al., 2017). A retrospective research found that 54.7% of the patients with TS had iatrogenic causes (Gelbard et al., 2015). Meanwhile, aging, obesity, and diabetes are also risk factors for TS (Li et al., 2018). However, the molecular mechanisms of TS have not been elucidated. And the diagnosis of TS is usually made after discharge, affecting the therapeutic effect (Shadmehr et al., 2017). Therefore, it is important to find the pathogenesis of TS for the early diagnosis and targeted therapy. Bioinformatics methods can be used to explore DEGs between TS and normal individuals. Through further analysis, multiple hub genes were found, of which *MKI67*, *CCNB1*, and *CCNB2* are worth paying attention.

MKI67, the marker of proliferation Ki-67, is mainly involved in regulating protein binding, DNA binding, regulation in mitotic nuclear division, cell proliferation, and regulation of chromosome segregation. What is more, *MKI67* might be involved in the occurrence of many diseases. Tokarz found that overexpression of MKI67 was accompanied by inflammatory stress and cell death, suggesting that *MKI67* may be involved in the process of cell cycle and proliferation (Tokarz, Piastowska-Ciesielska, Kaarniranta, & Blasiak, 2016). Hou found that knocking out *MKI67* can inhibit the growth of cancer cells, suggesting that *MKI67* may take part in cell division, and then affect the cell cycle (Hou et al., 2011). Similarly, through gene sequencing and association analysis, Yang suggested that *MKI67* and *TP53(OMIM: 191170)* may serve as molecular markers for cell cycle regulation (Yang et al., 2017). Xiong retrospectively analyzed multiple studies of 7,078 patients and found that high expression of *MKI67* reduced the overall survival rate and tumor-free survival

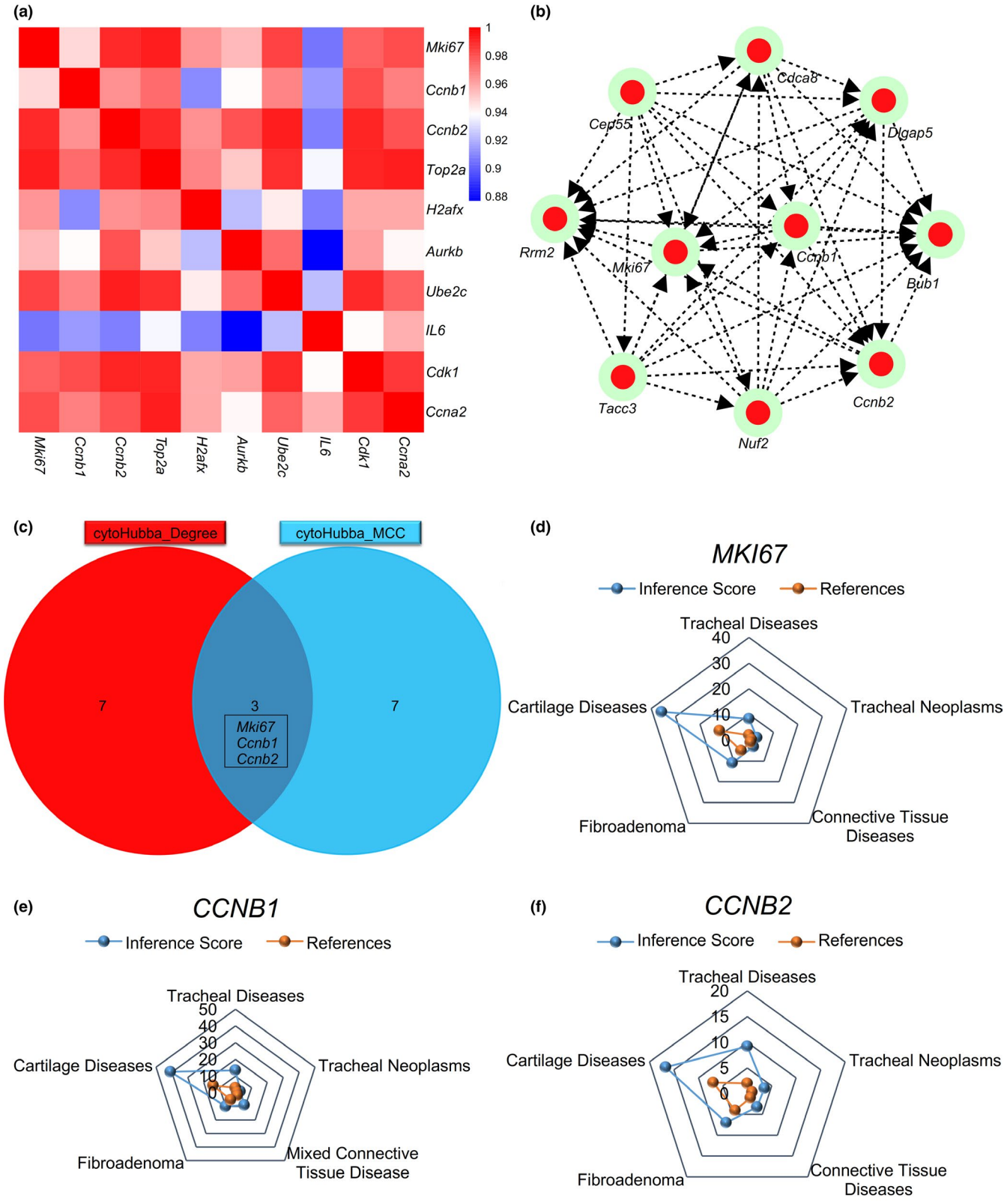

FIGURE 5 (a) The Pearson correlation analysis manifested that there exist positive correlations among these hub genes via cytoHubba_Degree. (b) The hub genes network via cytoHubba_MCC. (c) The VENN diagram between "cytoHubba_Degree" and "cytoHubba_MCC." (d) Relationship with trachea related to *MKI67* based on the CTD database. (e) Relationship with trachea related to *CCNB1* based on the CTD database. (f) Relationship with trachea related to *CCNB2* based on the CTD database. Note: *MKI67* (Reference Sequence: NG_047061.1), *CCNB1* (Reference Sequence: NC_000005.10), *CCNB2* (Reference Sequence: NC_000015.10)

rate. Further functional analysis revealed that *MKI67* might take part in the occurrence of apoptosis by regulating the p53 signaling pathway (Xiong, Zeng, Jiang, Luo, & Chen, 2019). Furthermore, Zeng demonstrated that *SNRPA1 (OMIM: 603521)* can regulate *PIK3R1 (OMIM:171833)*, *VEGFC (OMIM:601528)*, and *MKI67* molecules in colorectal cancer through gene overexpression and gene knockout experiments, and then be involved in tumorigenesis and development, suggesting that *MKI67* may serve as a molecular target for cell cycle and apoptosis (Zeng et al., 2019). Consistent with the above studies, we found that *MKI67* is highly expressed in TS tissues. We speculated that *MKI67* may promote tracheal endothelial cell proliferation and fibrosis by affecting the cell cycle, inducing scar tissue hyperplasia and then TS. *MKI67* might serve as a target for specific therapy of TS, and the relevant mechanisms are worth further exploration.

CCNB1, cyclin B1, is mainly involved in the cell cycle. Abnormal expression of *CCNB1* might lead to various diseases. Liu found that the polymorphism of *CCNB1* was significantly related with the efficacy of platinum-based chemotherapy. The polymorphism of *CCNB1* may be involved in the gastrointestinal toxicity of platinum-based chemotherapy. Further analysis suggests that *CCNB1* might regulate the cell cycle and G2/M phase, providing new ideas for individual treatment of patients with non–small-cell lung cancer (Liu et al., 2017). What is more, Zhang found that *CCNB1* was highly expressed in pancreatic cancer tissues by quantitative detection. *CCNB1* might affect pancreatic cancer cell cycle, proliferation and apoptosis through *TP53* pathway (Zhang, Feng, et al., 2018; Zhang, Zhang, et al., 2018). In addition, Gu found that inhibition of *CCNB1* expression could significantly inhibit the proliferation, migration, and invasion of cells (Gu, Liu, Li, & He, 2019). Li found that *CCNB1* could affect the proliferation and apoptosis of pituitary adenoma cells and activate epithelial-to-mesenchymal transition. Knockout of the *CCNB1* gene could inhibit cell proliferation (Li et al., 2019), suggesting that *CCNB1* could regulate cell cycle and affect cell proliferation. Furthermore, *CCNB1* is involved in regulating autophagy (Lu et al., 2019), which in turn regulates the degree of tissue fibrosis (Qin et al., 2017). Apoptosis of tracheal epithelial cells can promote the proliferation of fibroblasts, thereby aggravating TS

TABLE 2 Clinical variables and expression status of *MKI67*, *CCNB1*, and *CCNB2*

	Diagnosis		
Characteristics	**Tracheal stenosis**	**Control**	***p*-value**
Sex _ Male	10 (40.0%)	10 (40.0%)	.227
Sex _ Female	4 (16.0%)	1 (4.0%)	
Age (years old)	47.36 ± 18.44	59.64 ± 14.65	.076
Height (cm)	169.82 ± 3.68	165.64 ± 5.84	.050
Weight (kg)	74.96 ± 8.43	73.00 ± 9.88	.606
MKI67	2.42 ± 0.59	0.61 ± 0.39	.000
CCNB1	4.14 ± 0.92	1.44 ± 0.36	.000
CCNB2	3.64 ± 0.55	0.78 ± 0.23	.000

Note: MKI67 (Reference Sequence: NG_047061.1), *CCNB1* (Reference Sequence: NC_000005.10), *CCNB2* (Reference Sequence: NC_000015.10).

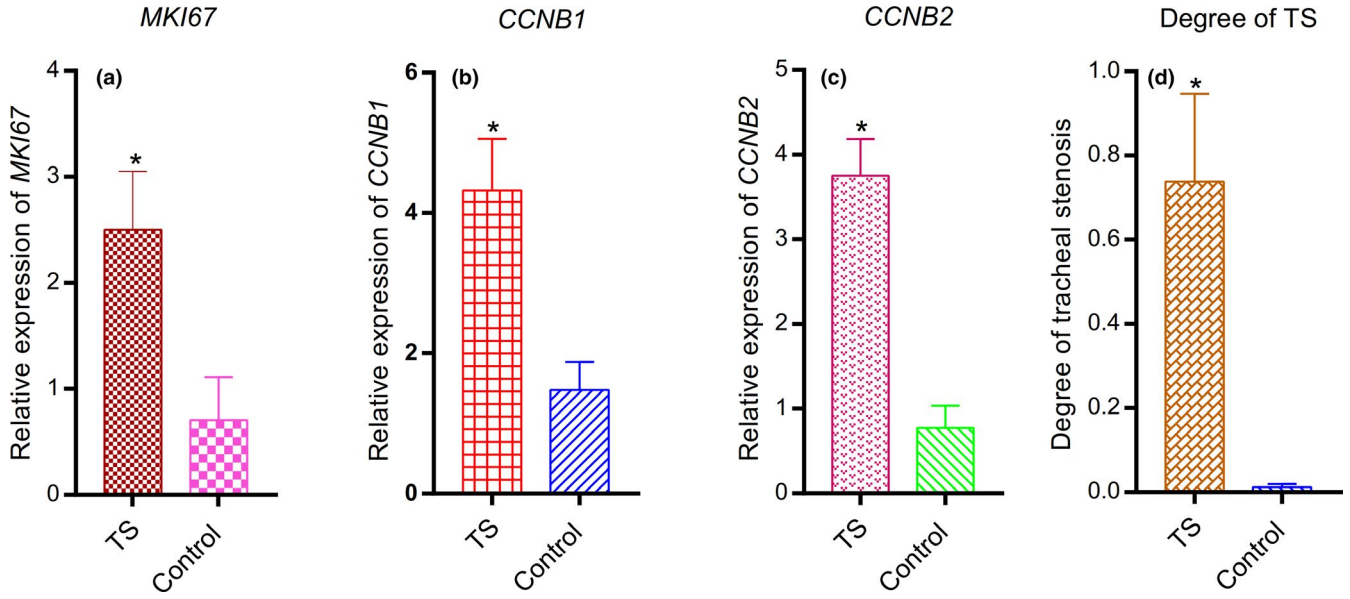

FIGURE 6 RT-qPCR analysis validation of the most significant genes, (a) *MKI67*, (b) *CCNB1*, and (c) *CCNB2*. (d) Comparison of degree of TS between TS and control groups. Note: *MKI67* (Reference Sequence: NG_047061.1), *CCNB1* (Reference Sequence: NC_000005.10), *CCNB2* (Reference Sequence: NC_000015.10)

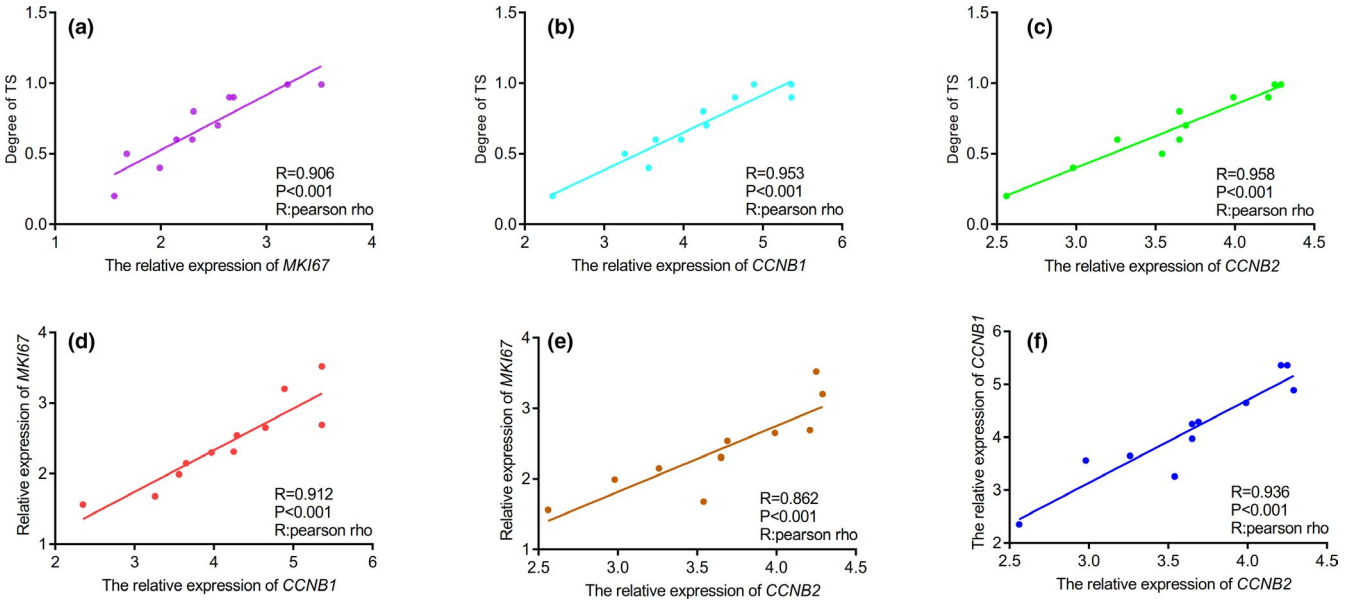

FIGURE 7 Strong positive associations between the degree of TS, *MKI67*, *CCNB1*, and *CCNB2* based on the Pearson correlation analysis. Note: *MKI67* (Reference Sequence: NG_047061.1), *CCNB1* (Reference Sequence: NC_000005.10), *CCNB2* (Reference Sequence: NC_000015.10)

(Wang et al., 2016). Consistent with the above studies, we found that *CCNB1* is highly expressed in TS tissues. We speculate that *CCNB1* may be involved in the occurrence and development of TS by regulating cell cycle, autophagy, and apoptosis. Overexpression of *CCNB1* can accelerate the cell cycle and promote endothelial proliferation, fibrosis, and hornification, then inducing TS. *CCNB1* may serve as a target for early diagnosis and specific therapy of tracheal stricture, and the related mechanisms need to be further studied.

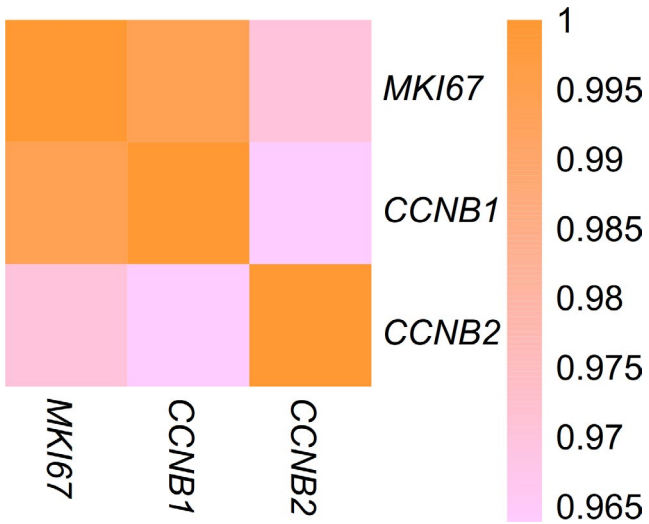

FIGURE 8 The heatmap presenting the correlation among the *MKI67*, *CCNB1*, and *CCNB2* based on the Spearman correlation analysis. Note: *MKI67* (Reference Sequence: NG_047061.1), *CCNB1* (Reference Sequence: NC_000005.10), *CCNB2* (Reference Sequence: NC_000015.10)

CCNB2, cyclin B2, is mainly involved in the regulation of growth, T-cell homeostasis, and cell cycle. Ian found significant overexpression of *CCNB2* in non–small-cell lung cancer tissues through bioinformatics analysis and quantitative validation, and the high expression of *CCNB2* protein can affect the overall survival rate of non–small-cell lung cancer patients, suggesting that *CCN B2* may be involved in the development of non–small cell lung cancer by regulating G2/M transition of cell cycle (Qian et al., 2015). What is more, Shi found that Islet-1 can regulate the expression of *CCNB2*, and then promote cell cycle progression of gastric cancer (GC) cells. In this study, the proportion of cells in the G1 phase is reduced, and the proportion of cells in the G2/M and S phases is increased, thereby promoting the proliferation of GC cells and providing new evidence for the study of the mechanisms of GC (Shi et al., 2016). In addition, Gao found that *KPNA2 (OMIM: 600685)* can upregulate the expression of *CCNB2*, and then induce the proliferation of hepatoma cells, thereby promoting the development of hepatoma, suggesting that related molecules can serve as therapeutic targets (Gao, Wang, Yang, Yang, & Zhuang, 2018). Furthermore, Wang found multiple genes differentially expressed in scar tissues and normal tissues through bioinformatics analysis. And through further analysis, Wang found that *CCNB2* may be involved in the development of scar by regulating the *TP53* signaling pathway, providing ideas for the study of the mechanisms of scar (Zeng et al., 2019). Consistent with the above studies, we found that *CCNB2* was highly expressed in TS. We speculate that *CCNB2* may be involved in the occurrence and development of TS by regulating cell cycle, inflammatory factors and inducing airway epithelial cell proliferation, fibrosis, and scar formation. *CCNB2* may serve as a target for early diagnosis

and specific therapy of tracheal stricture, and the related molecular mechanisms need to be further clarified.

However, there were some shortcomings. The small sample size in the dataset still needs to be further expanded to obtain more accurate results to better understand the molecular mechanisms of TS.

In summary, there are many DEGs between TS and normal tracheal tissues, especially *MKI67*, *CCNB1*, and *CCNB2*. These molecules might be molecular targets for early diagnosis and specific therapy of TS.

ACKNOWLEDGMENTS

We are thankful to Qing-qing Wang for her statistical assistance. This work was supported by the Chinese Academy of Sciences-Wego Group Hightech Research & Development Program (2019-1); and the Discipline Leader Training Program of Hebei Provincial Government (2018).

CONFLICT OF INTEREST

The authors declare they have no conflict of interest.

AUTHOR CONTRIBUTION

Conceptualization, Methodology: Lining Huang, Wenping Song. Data curation, Formal analysis, Investigation: Yong Qiu, Shu-xian Ma. Project administration, Resources, Software: Wen-hao Wu, Pei Zhang. Validation, Visualization: Ling-bing Meng, Wei Yang. Writing-original draft, Writing-review & editing: Xu-ze Li, Zi-chen Wang. All authors read and approved the final manuscript.

DATA AVAILABILITY STATEMENT

All data included in this study are available upon request by contact with the corresponding author.

ORCID

Lining Huang https://orcid.org/0000-0001-5754-2706

REFERENCES

Ahn, H. Y., Su, C. J., Kim, Y. D., & I, H. (2015). Surgical outcomes of post intubational or post tracheostomy tracheal stenosis: Report of 18 cases in single institution. *Annals of Thoracic and Cardiovascular Surgery*, *21*(1), 14–17. https://doi.org/10.5761/atcs.oa.13-00335

Ashburner, M., Ball, C. A., Blake, J. A., Botstein, D., Butler, H., Cherry, J. M., … Sherlock, G. (2000). Gene ontology: Tool for the unification of biology. *The Gene Ontology Consortium. Nature Genetics*, *25*(1), 25–29. https://doi.org/10.1038/75556

Bader, G. D., & Hogue, C. W. (2003). An automated method for finding molecular complexes in large protein interaction networks. *BMC Bioinformatics*, *4*, 2.

Chin, C. H., Chen, S. H., Wu, H. H., Ho, C. W., Ko, M. T., & Lin, C. Y. (2014). cytoHubba: Identifying hub objects and sub-networks from complex interactome. *BMC Systems Biology*, *8*(Suppl. 4), S11. https://doi.org/10.1186/1752-0509-8-S4-S11

D'Andrilli, A., Venuta, F., & Rendina, E. A. (2016). Subglottic tracheal stenosis. *Journal of Thoracic Disease*, *8*(Suppl. 2), S140–147.

Edgar, R., Domrachev, M., & Lash, A. E. (2002). Gene Expression Omnibus: NCBI gene expression and hybridization array data repository. *Nucleic Acids Research*, *30*(1), 207–210. https://doi.org/10.1093/nar/30.1.207

Farzanegan, R., Feizabadi, M., Ghorbani, F., Movassaghi, M., Vaziri, E., Zangi, M., … Shadmehr, M. B. (2017). An overview of tracheal stenosis research trends and hot topics. *Archives of Iranian Medicine*, *20*(9), 598–607.

Gao, C. L., Wang, G. W., Yang, G. Q., Yang, H., & Zhuang, L. (2018). Karyopherin subunit-alpha 2 expression accelerates cell cycle progression by upregulating CCNB2 and CDK1 in hepatocellular carcinoma. *Oncology Letters*, *15*(3), 2815–2820.

Gelbard, A., Francis, D. O., Sandulache, V. C., Simmons, J. C., Donovan, D. T., & Ongkasuwan, J. (2015). Causes and consequences of adult laryngotracheal stenosis. *The Laryngoscope*, *125*(5), 1137–1143. https://doi.org/10.1002/lary.24956

Gu, J., Liu, X., Li, J., & He, Y. (2019). MicroRNA-144 inhibits cell proliferation, migration and invasion in human hepatocellular carcinoma by targeting CCNB1. *Cancer Cell International*, *19*, 15. https://doi.org/10.1186/s12935-019-0729-x

Hou, Y. Y., Cao, W. W., Li, L., Li, S. P., Liu, T., Wan, H. Y., … Tang, H. (2011). MicroRNA-519d targets MKi67 and suppresses cell growth in the hepatocellular carcinoma cell line QGY-7703. *Cancer Letters*, *307*(2), 182–190. https://doi.org/10.1016/j.canlet.2011.04.002

Huang, D. W., Sherman, B. T., Tan, Q., Collins, J. R., Alvord, W. G., Roayaei, J., … Lempicki, R. A. (2007). The DAVID gene functional classification tool: A novel biological module-centric algorithm to functionally analyze large gene lists. *Genome Biology*, *8*(9), R183. https://doi.org/10.1186/gb-2007-8-9-r183

Kim, S. S., Khalpey, Z., Hsu, C., & Little, A. G. (2017). Changes in tracheostomy- and intubation-related tracheal stenosis: Implications for surgery. *The Annals of Thoracic Surgery*, *104*(3), 964–970. https://doi.org/10.1016/j.athoracsur.2017.03.063

Li, B., Zhu, H. B., Song, G. D., Cheng, J. H., Li, C. Z., Zhang, Y. Z., & Zhao, P. (2019). Regulating the CCNB1 gene can affect cell proliferation and apoptosis in pituitary adenomas and activate epithelial-to-mesenchymal transition. *Oncology Letters*, *18*(5), 4651–4658. https://doi.org/10.3892/ol.2019.10847

Li, M., Yiu, Y., Merrill, T., Yildiz, V., deSilva, B., & Matrka, L. (2018). Risk factors for posttracheostomy tracheal stenosis. Otolaryngology–head and neck surgery. *Otolaryngology-Head and Neck Surgery*, *159*(4), 698–704. https://doi.org/10.1177/0194599818794456

Lin, Z., Jaberi-Douraki, M., He, C., Jin, S., Yang, R. S. H., Fisher, J. W., & Riviere, J. E. (2017). Performance assessment and translation of physiologically based pharmacokinetic models from acslX to Berkeley Madonna, MATLAB, and R language: Oxytetracycline and gold nanoparticles as case examples. *Toxicological Sciences*, *158*(1), 23–35. https://doi.org/10.1093/toxsci/kfx070

Liu, D., Xu, W., Ding, X., Yang, Y., Su, B., & Fei, K. (2017). Polymorphisms of CCNB1 associated with the clinical outcomes of platinum-based chemotherapy in Chinese NSCLC patients. *Journal of Cancer*, *8*(18), 3785–3794.

Liu, J., Zhu, H., Wang, H., Li, J., Han, F., Liu, Y., … Hu, D. (2018). Methylation of secreted frizzled-related protein 1 (SFRP1) promoter downregulates Wnt/beta-catenin activity in keloids. *Journal of Molecular Histology*, *49*(2), 185–193.

Lu, G., Yi, J., Gubas, A., Wang, Y.-T., Wu, Y., Ren, Y. I., … Shen, H.-M. (2019). Suppression of autophagy during mitosis via CUL4-RING

ubiquitin ligases-mediated WIPI2 polyubiquitination and proteasomal degradation. *Autophagy*, *15*(11), 1917–1934. https://doi.org/10.1080/15548627.2019.1596484

Musah, S., Chen, J., Schlueter, C., Humphrey, D. M. Jr, Stocke, K., Hoyle, M. I., & Hoyle, G. W. (2019). Inhibition of chlorine-induced airway fibrosis by budesonide. *Toxicology and Applied Pharmacology*, *363*, 11–21. https://doi.org/10.1016/j.taap.2018.08.024

Qian, X., Song, X., He, Y., Yang, Z., Sun, T., Wang, J., … You, C. (2015). CCNB2 overexpression is a poor prognostic biomarker in Chinese NSCLC patients. *Biomedicine & Pharmacotherapy*, *74*, 222–227. https://doi.org/10.1016/j.biopha.2015.08.004

Qin, E. Y., Gan, L. M., Gan, J. H., Li, Y., Li, W. T., Hou, C. C., … Liu, G. N. (2017). Expression and significance of autophagy in rabbit model of tracheal stenosis. *Zhonghua Yi Xue Za Zhi*, *97*(48), 3816–3820.

Raghuraman, G., Rajan, S., Marzouk, J. K., Mullhi, D., & Smith, F. G. (2005). Is tracheal stenosis caused by percutaneous tracheostomy different from that by surgical tracheostomy. *Chest*, *127*(3), 879–885. https://doi.org/10.1378/chest.127.3.879

Ringner, M. (2008). What is principal component analysis. *Nature Biotechnology*, *26*(3), 303–304. https://doi.org/10.1038/nbt0308-303

Shadmehr, M. B., Abbasidezfouli, A., Farzanegan, R., Pejhan, S., Daneshvar, K. A., Sheikhy, K., … Zangi, M. (2017). The role of systemic steroids in postintubation tracheal stenosis: A randomized clinical trial. *The Annals of Thoracic Surgery*, *103*(1), 246–253. https://doi.org/10.1016/j.athoracsur.2016.05.063

Shi, Q., Wang, W., Jia, Z., Chen, P., Ma, K., & Zhou, C. (2016). ISL1, a novel regulator of CCNB1, CCNB2 and c-MYC genes, promotes gastric cancer cell proliferation and tumor growth. *Oncotarget*, *7*(24), 36489–36500.

Smith, M. M., & Cotton, R. T. (2018). Diagnosis and management of laryngotracheal stenosis. *Expert Review of Respiratory Medicine*, *12*(8), 709–717. https://doi.org/10.1080/17476348.2018.1495564

Smoot, M. E., Ono, K., Ruscheinski, J., Wang, P. L., & Ideker, T. (2011). Cytoscape 2.8: New features for data integration and network visualization. *Bioinformatics*, *27*(3), 431–432. https://doi.org/10.1093/bioinformatics/btq675

Su, Z., Li, S., Zhou, Z., Chen, X., Gu, Y., Chen, Y., … Zhong, N. (2017). A canine model of tracheal stenosis induced by cuffed endotracheal intubation. *Scientific Reports*, *7*, 45357. https://doi.org/10.1038/srep45357

Szklarczyk, D., Franceschini, A., Wyder, S., Forslund, K., Heller, D., Huerta-Cepas, J., … von Mering, C. (2015). STRING v10: Protein-protein interaction networks, integrated over the tree of life. *Nucleic Acids Research*, *43*(Database issue), D447–D452. https://doi.org/10.1093/nar/gku1003

Tanabe, M., & Kanehisa, M. (2012). Using the KEGG database resource. *Current Protocols in Bioinformatics*, *38*(1), https://doi.org/10.1002/0471250953.bi0112s38

Tokarz, P., Piastowska-Ciesielska, A. W., Kaarniranta, K., & Blasiak, J. (2016). All-Trans Retinoic Acid Modulates DNA Damage Response and the Expression of the VEGF-A and MKI67 Genes in ARPE-19 Cells Subjected to Oxidative Stress. *International Journal of Molecular Sciences*, *17*(6). https://doi.org/10.3390/ijms17060898

Wang, C., Xia, T., Jiang, K., Qiao, X., Zhang, X., Li, J., … Nie, J. (2016). Apoptosis of the tracheal epithelium can increase the number of recipient bone marrow-derived myofibroblasts in allografts and exacerbate obliterative bronchiolitis after tracheal transplantation in mice. *Transplantation*, *100*(9), 1880–1888. https://doi.org/10.1097/TP.0000000000001230

Wright, C. D., Li, S., Geller, A. D., Lanuti, M., Gaissert, H. A., Muniappan, A., … Mathisen, D. J. (2019). Postintubation tracheal stenosis: Management and results 1993 to 2017. *The Annals of Thoracic Surgery*, *108*(5), 1471–1477. https://doi.org/10.1016/j.athoracsur.2019.05.050

Xiong, D. D., Zeng, C. M., Jiang, L., Luo, D. Z., & Chen, G. (2019). Ki-67/MKI67 as a predictive biomarker for clinical outcome in gastric cancer patients: An updated meta-analysis and systematic review involving 53 studies and 7078 patients. *Journal of Cancer*, *10*(22), 5339–5354. https://doi.org/10.7150/jca.30074

Yang, C. K., Yu, T. D., Han, C. Y., Qin, W., Liao, X. W., Yu, L., … Peng, T. (2017). Genome-wide association study of MKI67 expression and its clinical implications in HBV-related hepatocellular carcinoma in Southern China. *Cellular Physiology and Biochemistry*, *42*(4), 1342–1357. https://doi.org/10.1159/000478963

Yin, L. X., Motz, K. M., Samad, I., Duvvuri, M., Murphy, M., Ding, D., & Hillel, A. T. (2017). Fibroblasts in hypoxic conditions mimic laryngotracheal stenosis. *Otolaryngology–head and Neck Surgery*, *156*(5), 886–892. https://doi.org/10.1177/0194599817697049

Zeng, Q., Lei, F., Chang, Y., Gao, Z., Wang, Y., Gao, Q., … Li, Q. (2019). An oncogenic gene, SNRPA1, regulates PIK3R1, VEGFC, MKI67, CDK1 and other genes in colorectal cancer. *Biomedicine & Pharmacotherapy*, *117*, 109076.

Zhang, H., Zhang, X., Li, X., Meng, W. B., Bai, Z. T., Rui, S. Z., … Jin, X. D. (2018). Effect of CCNB1 silencing on cell cycle, senescence, and apoptosis through the p53 signaling pathway in pancreatic cancer. *Journal of Cellular Physiology*, *234*(1), 619–631. https://doi.org/10.1002/jcp.26816

Zhang, X., Feng, H., Li, D., Liu, S., Amizuka, N., & Li, M. (2018). Identification of differentially expressed genes induced by aberrant methylation in oral squamous cell carcinomas using integrated bioinformatic analysis. *International Journal of Molecular Sciences*, *19*(6). https://doi.org/10.3390/ijms19061698

Zhou, Y., Zhou, B., Pache, L., Chang, M., Khodabakhshi, A. H., Tanaseichuk, O., … Chanda, S. K. (2019). Metascape provides a biologist-oriented resource for the analysis of systems-level datasets. *Nature Communications*, *10*(1), 1523. https://doi.org/10.1038/s41467-019-09234-6

How to cite this article: Li X-Z, Wang Z-C, Qiu Y, et al. Bioinformatics analysis and verification of gene targets for benign tracheal stenosis. *Mol Genet Genomic Med*. 2020;8:e1245. https://doi.org/10.1002/mgg3.1245